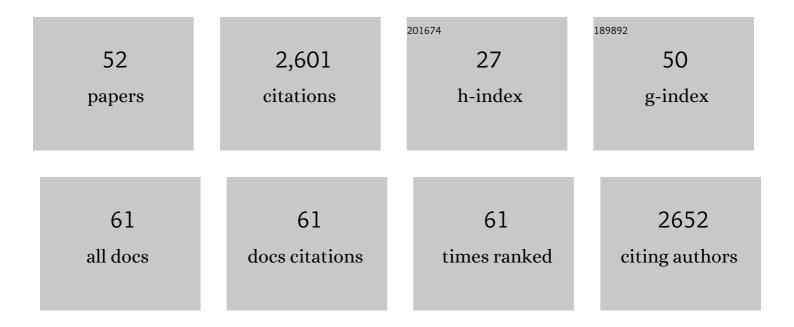
Shuo-Qing Zhang

List of Publications by Year in descending order

Source: https://exaly.com/author-pdf/6040715/publications.pdf Version: 2024-02-01



#	Article	IF	CITATIONS
1	Pd(ii)-catalyzed alkoxylation of unactivated C(sp3)–H and C(sp2)–H bonds using a removable directing group: efficient synthesis of alkyl ethers. Chemical Science, 2013, 4, 4187.	7.4	280
2	Pd(ii)-catalyzed alkylation of unactivated C(sp3)–H bonds: efficient synthesis of optically active unnatural α-amino acids. Chemical Science, 2013, 4, 3906.	7.4	202
3	Stereoselective Synthesis of Chiral β-Fluoro α-Amino Acids via Pd(II)-Catalyzed Fluorination of Unactivated Methylene C(sp ³)–H Bonds: Scope and Mechanistic Studies. Journal of the American Chemical Society, 2015, 137, 8219-8226.	13.7	183
4	Mechanisms and Origins of Chemo- and Regioselectivities of Ru(II)-Catalyzed Decarboxylative C–H Alkenylation of Aryl Carboxylic Acids with Alkynes: A Computational Study. Journal of the American Chemical Society, 2017, 139, 7224-7243.	13.7	134
5	Copperâ€Catalyzed Enantioselective Markovnikov Protoboration of αâ€Olefins Enabled by a Buttressed Nâ€Heterocyclic Carbene Ligand. Angewandte Chemie - International Edition, 2018, 57, 1376-1380.	13.8	129
6	Tuning the LUMO Energy of an Organic Interphase to Stabilize Lithium Metal Batteries. ACS Energy Letters, 2019, 4, 644-650.	17.4	129
7	Alternate Heme Ligation Steers Activity and Selectivity in Engineered Cytochrome P450-Catalyzed Carbene-Transfer Reactions. Journal of the American Chemical Society, 2018, 140, 16402-16407.	13.7	106
8	Mechanism and Origins of Ligand-Controlled Stereoselectivity of Ni-Catalyzed Suzuki–Miyaura Coupling with Benzylic Esters: AÂComputational Study. Journal of the American Chemical Society, 2017, 139, 12994-13005.	13.7	99
9	Nucleophile-Dependent <i>Z</i> / <i>E</i> - and Regioselectivity in the Palladium-Catalyzed Asymmetric Allylic C–H Alkylation of 1,4-Dienes. Journal of the American Chemical Society, 2019, 141, 5824-5834.	13.7	89
10	Palladium-Catalyzed Selective Five-Fold Cascade Arylation of the 12-Vertex Monocarborane Anion by B–H Activation. Journal of the American Chemical Society, 2018, 140, 13798-13807.	13.7	79
11	A general and practical palladium-catalyzed monoarylation of β-methyl C(sp3)–H of alanine. Chemical Communications, 2014, 50, 13924-13927.	4.1	78
12	Stereoselective alkoxycarbonylation of unactivated C(sp3)–H bonds with alkyl chloroformates via Pd(II)/Pd(IV) catalysis. Nature Communications, 2016, 7, 12901.	12.8	66
13	Redox-Activated Light-Up Nanomicelle for Precise Imaging-Guided Cancer Therapy and Real-Time Pharmacokinetic Monitoring. ACS Nano, 2016, 10, 11385-11396.	14.6	65
14	Predicting Regioselectivity in Radical Câ^'H Functionalization of Heterocycles through Machine Learning. Angewandte Chemie - International Edition, 2020, 59, 13253-13259.	13.8	65
15	Stereoretentive C(<i>sp</i> ³)–S Cross-Coupling. Journal of the American Chemical Society, 2018, 140, 18140-18150.	13.7	55
16	Practical Synthesis of <i>anti</i> â€Î²â€Hydroxyâ€Î±â€Amino Acids by Pd ^{ll} â€Catalyzed Sequential C(sp ³)H Functionalization. Chemistry - A European Journal, 2015, 21, 3264-3270.	3.3	53
17	Rhodium(III)-Catalyzed Asymmetric Borylative Cyclization of Cyclohexadienone-Containing 1,6-Dienes: An Experimental and DFT Study. Journal of the American Chemical Society, 2019, 141, 12770-12779.	13.7	52
18	Divergent rhodium-catalyzed electrochemical vinylic C–H annulation of acrylamides with alkynes. Nature Communications, 2021, 12, 930.	12.8	48

Shuo-Qing Zhang

#	Article	IF	CITATIONS
19	Catalytic asymmetric synthesis of chiral trisubstituted heteroaromatic allenes from 1,3-enynes. Communications Chemistry, 2018, 1, .	4.5	43
20	A Unified Explanation for Chemoselectivity and Stereospecificity of Ni-Catalyzed Kumada and Cross-Electrophile Coupling Reactions of Benzylic Ethers: A Combined Computational and Experimental Study. Journal of the American Chemical Society, 2019, 141, 5835-5855.	13.7	41
21	Palladium(0)-catalyzed cyclopropanation of benzyl bromides via C(sp ³)–H bond activation. Chemical Communications, 2014, 50, 3692-3694.	4.1	39
22	Catalytic and Photochemical Strategies to Stabilized Radicals Based on Anomeric Nucleophiles. Journal of the American Chemical Society, 2020, 142, 11102-11113.	13.7	39
23	Computational studies on Ni-catalyzed amide C–N bond activation. Chemical Communications, 2019, 55, 11330-11341.	4.1	37
24	Diastereoselective olefin amidoacylation <i>via</i> photoredox PCET/nickel-dual catalysis: reaction scope and mechanistic insights. Chemical Science, 2020, 11, 4131-4137.	7.4	37
25	Copper atalyzed Enantioselective Markovnikov Protoboration of αâ€Olefins Enabled by a Buttressed Nâ€Heterocyclic Carbene Ligand. Angewandte Chemie, 2018, 130, 1390-1394.	2.0	36
26	Mechanism and Selectivity Control in Ni- and Pd-Catalyzed Cross-Couplings Involving Carbon–Oxygen Bond Activation. Accounts of Chemical Research, 2021, 54, 2158-2171.	15.6	33
27	Coulombic-enhanced hetero radical pairing interactions. Nature Communications, 2018, 9, 1961.	12.8	30
28	Mechanism and Origins of Chemo- and Regioselectivities of Pd-Catalyzed Intermolecular σ-Bond Exchange between Benzocyclobutenones and Silacyclobutanes: A Computational Study. Organometallics, 2018, 37, 592-602.	2.3	29
29	Rhodium-Catalyzed Asymmetric Addition of Organoboronic Acids to Aldimines Using Chiral Spiro Monophosphite-Olefin Ligands: Method Development and Mechanistic Studies. Journal of Organic Chemistry, 2018, 83, 11873-11885.	3.2	25
30	C–H Acidity and Arene Nucleophilicity as Orthogonal Control of Chemoselectivity in Dual C–H Bond Activation. Organic Letters, 2019, 21, 2360-2364.	4.6	24
31	Synthesis of chiral α-hydroxy acids via palladium-catalyzed C(sp ³)–H alkylation of lactic acid. Chemical Communications, 2016, 52, 1915-1918.	4.1	23
32	Engineered Cytochrome c-Catalyzed Lactone-Carbene B–H Insertion. Synlett, 2019, 30, 378-382.	1.8	22
33	Towards Dataâ€Driven Design of Asymmetric Hydrogenation of Olefins: Database and Hierarchical Learning. Angewandte Chemie - International Edition, 2021, 60, 22804-22811.	13.8	21
34	N-heterocyclic Carbene–Cu-Catalyzed Enantioselective Conjugate Additions with Alkenylboronic Esters as Nucleophiles. ACS Catalysis, 2017, 7, 5693-5698.	11.2	20
35	Carboxylate breaks the arene C–H bond <i>via</i> a hydrogen-atom-transfer mechanism in electrochemical cobalt catalysis. Chemical Science, 2020, 11, 5790-5796.	7.4	19
36	Aluminum-Catalyzed Selective Hydroboration of Alkenes and Alkynylsilanes. Organic Process Research and Development, 2019, 23, 1703-1708.	2.7	18

Shuo-Qing Zhang

#	Article	IF	CITATIONS
37	How Solvents Control the Stereospecificity of Ni-Catalyzed Miyaura Borylation of Allylic Pivalates. ACS Catalysis, 2019, 9, 9589-9598.	11.2	18
38	Palladium-catalyzed C(sp ³)–H arylation of lactic acid: efficient synthesis of chiral β-aryl-α-hydroxy acids. Organic Chemistry Frontiers, 2016, 3, 204-208.	4.5	17
39	N-Heterocyclic Carbene–Cu-Catalyzed Enantioselective Allenyl Conjugate Addition. Organic Letters, 2018, 20, 6896-6900.	4.6	14
40	Predicting Regioselectivity in Radical Câ^'H Functionalization of Heterocycles through Machine Learning. Angewandte Chemie, 2020, 132, 13355-13361.	2.0	14
41	Copperâ€Catalyzed Enantioselective Hydroboration of 1,1â€Disubstituted Alkenes: Method Development, Applications and Mechanistic Studies. Asian Journal of Organic Chemistry, 2018, 7, 103-106.	2.7	13
42	Enantioselective Intramolecular Desymmetric αâ€Addition of Cyclohexanone to Propiolamide Catalyzed by Sodium L â€Prolinate. Chinese Journal of Chemistry, 2019, 37, 63-70.	4.9	13
43	Machine learning prediction of hydrogen atom transfer reactivity in photoredox-mediated C–H functionalization. Organic Chemistry Frontiers, 2021, 8, 6187-6195.	4.5	12
44	An Unconventional <i>trans</i> - <i>exo</i> -Selective Cyclization of Alkyne-Tethered Cyclohexadienones Initiated by Rhodium(III)-Catalyzed C–H Activation via Insertion Relay. CCS Chemistry, 2021, 3, 1582-1595.	7.8	10
45	Understanding the mechanism and reactivity of Pd-catalyzed C–P bond metathesis of aryl phosphines: a computational study. Organic and Biomolecular Chemistry, 2020, 18, 5414-5419.	2.8	8
46	Understanding the Structureâ€Activity Relationship of Niâ€Catalyzed Amide Câ^'N Bond Activation using Distortion/Interaction Analysis. ChemCatChem, 2021, 13, 3536-3542.	3.7	8
47	Stepwise versus Concerted Reductive Elimination Mechanisms in the Carbon–lodide Bond Formation of (DPEphos)RhMel ₂ Complex. Organometallics, 2018, 37, 4711-4719.	2.3	7
48	Unexpected Stability of CO-Coordinated Palladacycle in Bidentate Auxiliary Directed C(sp ³)–H Bond Activation: A Combined Experimental and Computational Study. Organometallics, 2019, 38, 2022-2030.	2.3	6
49	Nickel-Catalyzed Domino Cross-Electrophile Coupling Dicarbofunctionalization Reaction To Afford Vinylcyclopropanes. ACS Catalysis, 2021, 11, 14369-14380.	11.2	5
50	Computation-Guided Development of the "Click―ortho-Quinone Methide Cycloaddition with Improved Kinetics. Organic Letters, 2020, 22, 2920-2924.	4.6	4
51	Towards Dataâ€Driven Design of Asymmetric Hydrogenation of Olefins: Database and Hierarchical Learning. Angewandte Chemie, 2021, 133, 22986-22993.	2.0	3
52	Divergent pathway and reactivity control of intramolecular arene C–H vinylation by vinyl cations. Organic and Biomolecular Chemistry, 2019, 17, 9135-9139.	2.8	1